

# RSC Advances



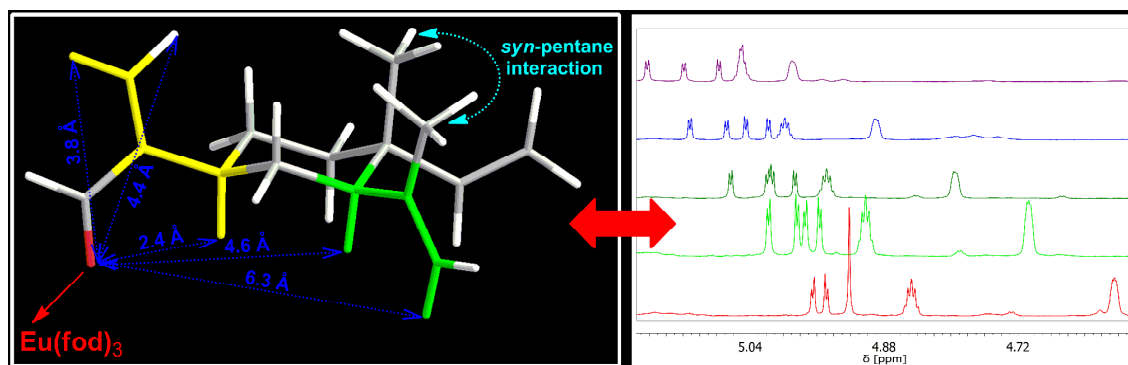
This is an *Accepted Manuscript*, which has been through the Royal Society of Chemistry peer review process and has been accepted for publication.

*Accepted Manuscripts* are published online shortly after acceptance, before technical editing, formatting and proof reading. Using this free service, authors can make their results available to the community, in citable form, before we publish the edited article. This *Accepted Manuscript* will be replaced by the edited, formatted and paginated article as soon as this is available.

You can find more information about *Accepted Manuscripts* in the [Information for Authors](#).

Please note that technical editing may introduce minor changes to the text and/or graphics, which may alter content. The journal's standard [Terms & Conditions](#) and the [Ethical guidelines](#) still apply. In no event shall the Royal Society of Chemistry be held responsible for any errors or omissions in this *Accepted Manuscript* or any consequences arising from the use of any information it contains.

A new approach to the structural elucidation of constituent(s) of complex mixtures was developed based on the use of lanthanide-induced shift reagents. This methodology was successfully applied in the identification of a rare sesquiterpene elemental.



1 Lanthanide-induced shift reagents enable structural elucidation of natural products in  
2 inseparable complex mixtures - The case of elemenal from *Inula helenium* L. (Asteraceae)<sup>†</sup>

3  
4 Marija S. Genčić and Niko S. Radulović\*

5  
6 *Department of Chemistry, Faculty of Science and Mathematics, University of Niš,*  
7 *Višegradaska 33, 18000, Niš, Serbia*

8  
9  
10 <sup>†</sup> Electronic supplementary information (ESI) available: A comparison of experimental and  
11 simulated <sup>1</sup>H NMR spectra of elemenal (the second order vinyl group spin system).

12  
13 \*Correspondence to: N. S. Radulović, Department of Chemistry, Faculty of Science and  
14 Mathematics, University of Niš, Višegradaska 33, 18000 Niš, Serbia. E-mail:  
15 [nikoradulovic@yahoo.com](mailto:nikoradulovic@yahoo.com); Tel.: +38118533015; Fax: +38118533014.

## 16 17 **Abstract**

18  
19 The use of lanthanide complexes for resolving intricate NMR signals and, in the case  
20 of chiral ligands, for determining enantiomeric excess has progressively decreased in the last  
21 30 years. Recently, a sesquiterpene aldehyde from *Inula helenium* with a possible potent  
22 antistaphylococcal activity remained unidentified due to the impossibility to separate the  
23 compound from its complex matrix available in very low amount (*ca.* 5 mg). Detailed  
24 analyses of 1D and 2D NMR spectra of this original complex sample allowed access to a very  
25 limited amount of structural data for the unknown aldehyde. We decided to investigate the  
26 potential usefulness of lanthanide-induced shift reagents for the resolution and assignment of  
27 overlapped <sup>1</sup>H NMR signals originating from different components of this complex mixture  
28 (*i.e.* for a qualitative analysis). The incremental addition of *tris*(6,6,7,7,8,8,8-heptafluoro-2,2-  
29 dimethyl-3,5-octanedionato)europium(III) (Eu(fod)<sub>3</sub>) led to a simplification of NMR spectra  
30 in terms of signal overlap and removal of chemical shift degeneracy, allowing the mining of  
31 crucial data from the shifted NMR spectra. 2D-NMR spectra (<sup>1</sup>H-<sup>1</sup>H-COSY, NOESY, HSQC  
32 and HMBC) of the sample mixed with Eu(fod)<sub>3</sub> proved to be particularly valuable in this  
33 respect. The obtained additional information revealed that the compound in question was a  
34 rare sesquiterpene - elemenal (elema-1,3,11(13)-trien-12-al). Therefore, herein we report on a  
35 new chromatography-free methodology that could be of value in structure elucidation of  
36 unknown compounds even if they are not available in pure state.

## 37 38 **Introduction**

39  
40 Nuclear magnetic resonance spectroscopy is one of the most powerful analytical  
41 techniques for the elucidation of structures of organic compounds. Continuous efforts have  
42 been made to develop different 1D-, 2D- and multidimensional-NMR methods in order to  
43 obtain more information from NMR measurements that will facilitate and accelerate structure  
44 determination. In general, it is considered that the structure of a new organic molecule is  
45 established if total assignment of <sup>1</sup>H and <sup>13</sup>C NMR data could be achieved. However, the  
46 application of these sophisticated NMR methods can sometimes, even if one has a fairly good  
47 idea of the likely structure, be insufficient to remove concerns regarding, for example, the  
48 position of certain substituent(s) or a double bond, relative stereochemistry or unequivocal  
49 assignment of all carbon or hydrogen atoms from so called overlapping signals. Most  
50 frequently these difficulties occur in the interpretation of complex or poorly-functionalized

1 (*i.e.* having a small number of highly electronegative heteroatoms) organic molecules (e.g.  
2 sterols, terpenes or lipids) as the signals, especially in  $^1\text{H}$  NMR spectra, are bunched together  
3 in featureless clusters from which little definitive structural information can be obtained. This  
4 occurrence of overlapping resonances of non-equivalent protons is a consequence of  
5 relatively low sensitivity of proton chemical shifts to changes in the chemical and  
6 stereochemical environments.<sup>1-3</sup> Nowadays, this problem could be solved, to some extent, by  
7 the advent of high-field NMR equipment, but the cost of this is often beyond the means of  
8 many spectroscopic departments.

9 Another approach to NMR spectra simplification, initially reported in 1969 by  
10 Hinckley<sup>4</sup> and extensively employed mostly in the next two decades, is the introduction of a  
11 lanthanide shift reagent (LSR). The application of LSRs is based on their ability to selectively  
12 coordinate electron-donor functional groups in the substrates and induce shifts of signals in  
13 NMR spectra.<sup>5</sup> The most common practice is to successively add known amounts of LSR to  
14 the compound under study and record NMR spectra after each addition (the shifted spectra).  
15 The chemical shifts of some protons and carbons in the substrates alter, to a greater or lesser  
16 degree, with each addition of LSR and may result in the segregation of overlapping signals  
17 that could facilitate its assignments.<sup>3</sup> This approach has been successfully employed in  
18 structural and conformational analysis of many synthetic organic compounds and natural  
19 products, as well as in the study of their chirality, but it requires the substrate in pure state  
20 with known or almost resolved structure on the basis of data from regular NMR  
21 measurements.<sup>1,5-11</sup> In recent years experiments involving chiral LSRs have been successfully  
22 carried out for the enantiomeric discrimination of oxygenated bicyclic monoterpenes (bornyl  
23 acetate, fenchone and camphor) contained in essential oils, without isolation of the  
24 compounds.<sup>12,13</sup> Similar methodology was applied in enantiomeric ratio determination of  
25 atropine and hyoscyamine in the crude extract of *Datura stramonium* seeds.<sup>14</sup>

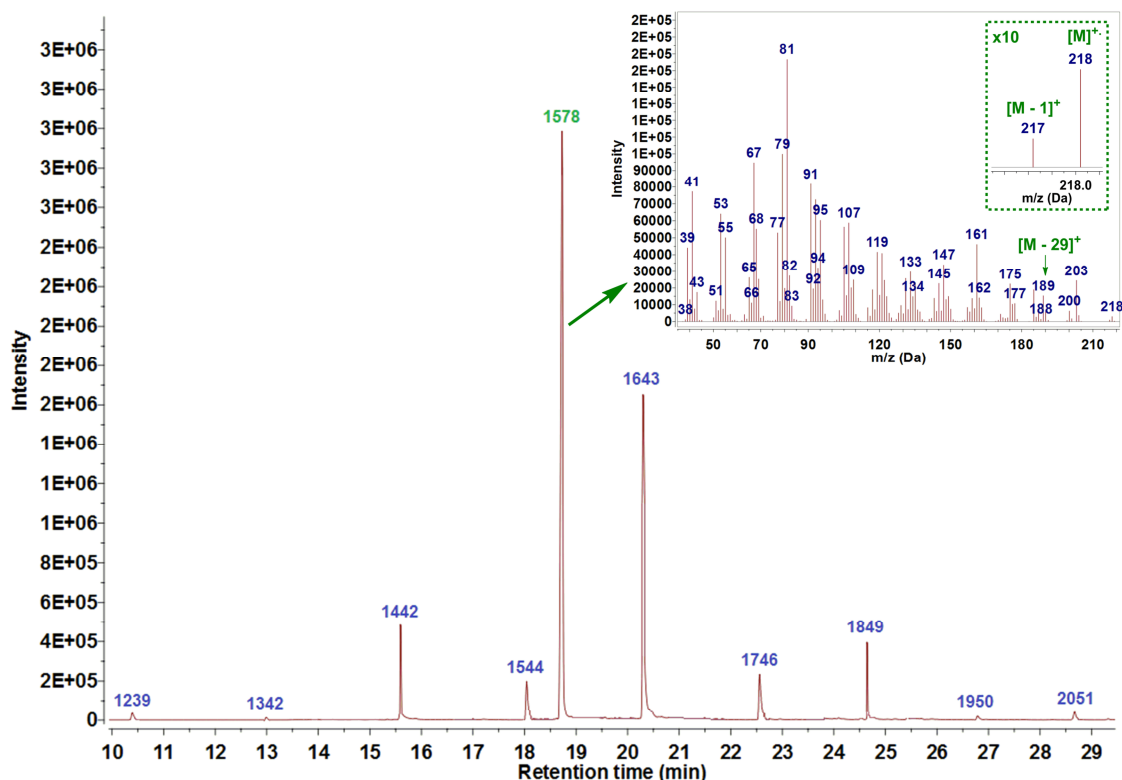
26 In the mentioned three quantitative studies,<sup>12-14</sup> where a particular compound was  
27 analyzed directly in a naturally occurring mixture, a standard of the compound in question  
28 was needed for the calibration curves set up and the methodologies were based on the  
29 existence of a set of non-overlapped (by the matrix molecules and the analytes) signals.  
30 Because of this, these researchers chose to track the lanthanide-induced shifts of  $^{13}\text{C}$  NMR  
31 signals, despite the loss of sensitivity and the onset of  $^{13}\text{C}$  NMR signal integration issues,  
32 since the proton decoupled  $^{13}\text{C}$  NMR spectrum is inherently less complex than the  $^1\text{H}$  NMR  
33 spectrum. Up to now, LSR methodology has not been used to resolve overlapped signals  
34 originating from different (non-enantiomeric) molecules (in both  $^1\text{H}$  and  $^{13}\text{C}$  NMR), let alone  
35 for the structural elucidation of individual unknown constituents in a mixture, *i.e.* for  
36 qualitative purposes. The resolution of accidentally overlapped signals from two or more  
37 different molecules could be a plausible outcome of a gradual addition of a LSR directly to  
38 the mixture since a distinct conduct of these signals is expected due to molecular differences  
39 (differing spatial relationship with the LSR complexing functional group and its identity),  
40 competitive complexation (differing stabilities of the LSR complexes of different mixture  
41 constituents) and shifting of the complexation equilibrium by different amounts of the  
42 individual constituents.<sup>2,3</sup>

43 Furthermore, there is only a handful of studies that combined 2D NMR ( $^1\text{H}$ - $^1\text{H}$   
44 COSY, NOESY, HSQC and HMBC) with LSR experiments in an attempt to perform a  
45 complete assignment of  $^1\text{H}$  NMR and  $^{13}\text{C}$  NMR resonances of natural products.<sup>15-17</sup> Also, the  
46 presence of LSR, that are paramagnetic in nature, should result in the increased  $^{13}\text{C}$  NMR  
47 sensitivity and shorten the time needed to acquire good quality spectra even for samples  
48 available in low amount.<sup>18</sup> This could have a downside, since nuclear Overhauser effect  
49 decreases (but does not disappear) under such conditions and at high LSR concentrations this

1 could lead to signal broadening. Therefore, to avoid the shortcomings, a titration with LSR is  
2 advised.<sup>2</sup>

3 Previously, in search for antimicrobial constituents of *Inula helenium* L.  
4 (Compositae), the activity of the plant essential oil was allocated to a minor chromatographic  
5 fraction composed of a series of 3-methyl-2-alkanones of varying chain lengths (C<sub>11</sub>–C<sub>19</sub>) and  
6 an unidentified sesquiterpene.<sup>19,20</sup> The identity of the 3-methyl-2-alkanones was confirmed by  
7 a synthetic approach based on the creation of a combinatorial library of such compounds  
8 since the amount and complexity of the fraction did not permit further chromatographic  
9 separation. This synthetic approach also allowed us to verify whether the ketones were  
10 responsible for the high noted antistaphylococcal activity. Unfortunately, the synthetic  
11 compounds turned out to be poor antimicrobial agents, hence indicating that the activity of  
12 the fraction originated from the mentioned unknown sesquiterpene. This compound showed  
13 the highest *m/z* value at 218 (molecular weight of an oxygenated sesquiterpene, C<sub>15</sub>H<sub>22</sub>O) in  
14 its mass spectrum, accompanied by recognizable ions, [M – 1]<sup>+</sup> and [M – 29]<sup>+</sup>, characteristic  
15 for aldehydes (Fig. 1), that resembled that of bicyclogermacrenal.<sup>20</sup>

16



17

18

19 **Fig. 1.** The original TIC chromatogram of a GC–MS run of a fraction (5% diethyl ether in  
20 hexane) of *I. helenium* root essential oil showing peaks with retention indices (blue colored)  
21 corresponding to a series of 3-methyl-2-alkanones and an unidentified sesquiterpene aldehyde  
22 (green colored) and the mass spectrum of the aldehyde.

23

24

25 In order to identify this sesquiterpene aldehyde, a larger quantity of the essential oil  
26 was fractionated by chromatography on SiO<sub>2</sub>. Repeated usage of a non-polar eluent led to  
27 sample A, which weighted *c.a.* 5 mg, enriched with the compound in question. The GC–MS  
28 analysis of this sample revealed that it contained roughly 85% of the sesquiterpene  
accompanied with geranyl (8%) and neryl isobutanoates (5%), as the main contaminants.

1 Furthermore, 1D and 2D NMR spectra of this sample were rather complex for interpretation  
2 and, hence uninformative, because of a number of overlapping signals originating from both  
3 the aldehyde and the contaminants. This mixture was an excellent candidate for the testing of  
4 the applicability of LSRs in structural elucidation of compounds in mixtures by the  
5 abovementioned simplification/resolution of 1D and 2D NMR spectra when further  
6 purification was not possible. Therefore, we decided to try to simplify the NMR spectra of  
7 this sample by an incremental introduction of  $\text{Eu}(\text{fod})_3$  in order to identify the mentioned  
8 sesquiterpene aldehyde. One can assume that the impact of LSR will be most obvious on the  
9 signals corresponding to this sesquiterpene as it is the major component of the mixture and  
10 has an aldehyde group that is very suitable for coordination of LSR.<sup>3</sup>

11 Thus, in this work, we report the successful identification and spectral  
12 characterisation of a sesquiterpene aldehyde from a complex sample representing a mixture  
13 of several compounds, without the isolation of the aldehyde in pure state, by the application  
14 of a new structural elucidation methodology based on the analyses of shifted 1D and 2D  
15 NMR spectra of the mentioned mixture.

16

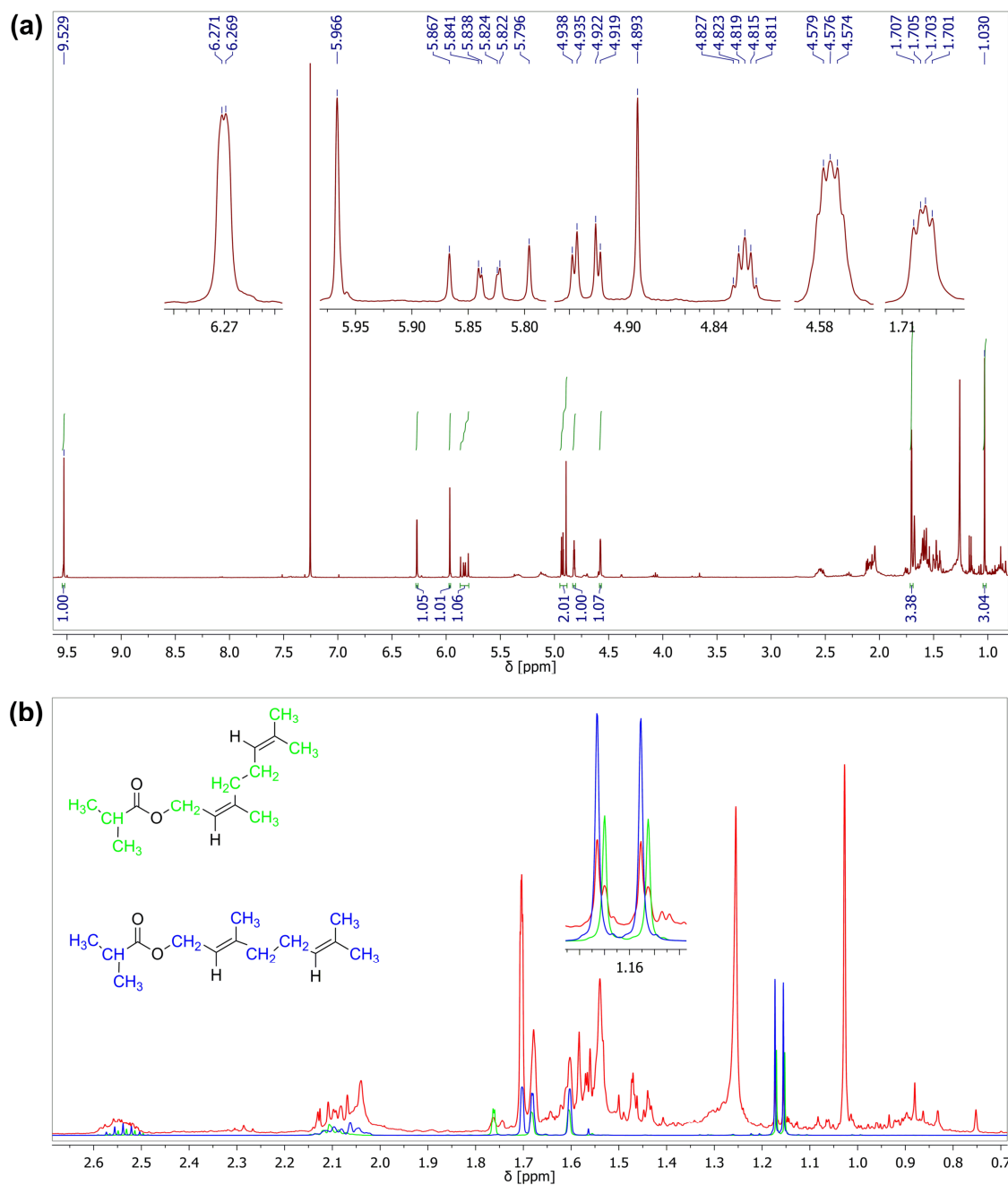
## 17 Results and discussion

18

19 Extensive NMR measurements of sample **A** were done in order to try to gain as much  
20 structural data on the sesquiterpene aldehyde as possible directly from the mixture (85% of  
21 the sesquiterpene accompanied with geranyl (8%) and neryl isobutanoates (5%)). Expectedly,  
22  $^1\text{H}$  NMR spectrum of sample **A** in deuterated chloroform exhibited a distinguishing broad  
23 singlet for an aldehyde proton at  $\delta_{\text{H}}$  9.53 (assigned an integral value of 1). This spectrum  
24 contained seven olefinic protons, at  $\delta_{\text{H}}$  6.27 (1H, br d,  $J = 0.7$  Hz), 5.97 (1H, br s), 5.83 (1H,  
25 m), 4.82 (1H, pseudo-quintet), 4.58 (1H, m) and two-proton second-order signal in the region  
26 4.88-4.95 ppm, that appeared to belong to the aldehyde according to the value of their  
27 integrals (Fig. 2a). Two low-intensity multiplets at 5.38-5.29 and 5.15-5.05 ppm were  
28 unambiguously confirmed to belong to the olefinic protons of the two main impurities,  
29 geranyl and neryl isobutanoates, by comparison with the corresponding chemical shifts in  $^1\text{H}$   
30 NMR spectra of authentic standards (Figs. 2a and 2b). Surprisingly, a complete assignment of  
31 the  $^1\text{H}$  and  $^{13}\text{C}$  resonances of the isobutanoates was lacking in the literature. The region of  $^1\text{H}$   
32 NMR spectrum up to 3 ppm was very complex to analyse since it contained a number of  
33 highly overlapped signals. The only peak that could be straightforwardly discerned was a  
34 singlet corresponding to a  $\text{CH}_3$  group at  $\delta_{\text{H}}$  1.03 (3H) attached to a quaternary carbon atom.

35 Alongside the aldehyde carbon atom signal at  $\delta_{\text{C}}$  194.5,  $^{13}\text{C}$  NMR spectrum exhibited  
36 eight olefinic signals, four of which having significantly higher intensities than the rest.  
37 DEPT135 spectrum showed that three of them, at  $\delta_{\text{C}}$  132.9, 112.2 and 110.1, corresponded to  
38 methylene groups ( $=\text{CH}_2$ ), while the remaining one at  $\delta_{\text{C}}$  150.0 was a methine olefinic carbon  
39 ( $=\text{CH}-$ ). This matches the number of proton resonances that were associated with the  
40 aldehyde mentioned above. Consequently, the aldehyde should have (at least) three double  
41 bonds with two olefinic carbons being non-protonated. This assumption was confirmed by  
42 appropriate cross peaks observed in the gHMQC spectrum: (i) the methine carbon signal at  
43 150.0 ppm correlated with the proton at  $\delta_{\text{H}}$  5.83 (ii) the methylene olefinic carbon at  $\delta_{\text{C}}$  132.9  
44 with protons at  $\delta_{\text{H}}$  6.27 and 5.97; (iii) the methylene olefinic carbon at  $\delta_{\text{C}}$  112.2 with protons  
45 at  $\delta_{\text{H}}$  4.82 and 4.58; (iv) while the methylene olefinic carbon at  $\delta_{\text{C}}$  110.1 seemed to correlate  
46 with both protons in the region 4.88-4.95 ppm. All three pairs of methylene olefinic protons  
47 showed cross peaks in the  $^1\text{H}-^1\text{H}$  gDQCOSY spectrum, as well. Additionally, the DEPT135  
48 spectrum revealed the presence of two methyl groups at 24.9 and 16.6 ppm that coupled in  
49 the gHMQC spectrum with the signals at  $\delta_{\text{H}}$  1.70 and 1.03, respectively. The singlet at 1.03  
50 ppm was already proposed to correspond to a  $\text{CH}_3$  group attached to a quaternary carbon

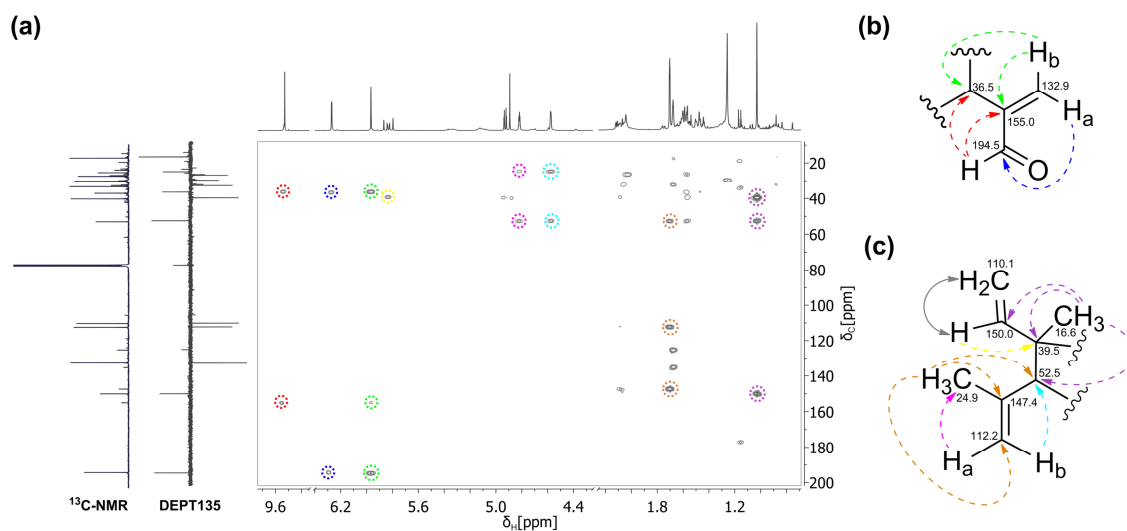
1 atom, but a closer inspection of  $^1\text{H}$  NMR spectrum in the region around 1.70 ppm allowed a  
 2 perception of another  $\text{CH}_3$  as a possible doublet of doublets ( $J = 1.6, 0.8$  Hz). Chemical  
 3 shifts,  $\delta_{\text{H}}$  1.70 and  $\delta_{\text{C}}$  24.9, for the second deshielded methyl group implied that it was most  
 4 probably attached to a double bonds.  
 5



6  
 7  
 8  
 9  
 10  
 11  
 12

**Fig. 2.** (a)  $^1\text{H}$  NMR spectrum of sample **A** with signals assigned to unknown sesquiterpene aldehyde. (b) Overlapping of  $^1\text{H}$  NMR spectrum (high field region) of sample **A** (marked red) with  $^1\text{H}$  NMR spectra of two main contaminants neryl isobutanoate (marked green) and geranyl isobutanoate (marked blue).

1 The correlations observed in  $^1\text{H}$ - $^{13}\text{C}$  gHMBC spectrum of sample **A** were very  
 2 informative and enabled the construction of two structural moieties presented in Fig. 3. The  
 3 geminal methylene protons at  $\delta_{\text{H}}$  6.27 and 5.97 had significantly different chemical shifts due  
 4 to an anisotropic effect of the aldehyde group. The proton  $\text{H}_a$  that resonated at lower field  
 5 was readily assigned to the proton *cis* to the aldehyde group. It demonstrated a relatively  
 6 resolved long-range coupling constant of 0.7 Hz, and most probably additional ones that led  
 7 to signal broadening. In this way an  $\alpha$ -substituted acrolein moiety was established (Fig. 3b).  
 8 The structure of the second fragment was deduced from a combination of data inferred from  
 9  $^1\text{H}$ - $^{13}\text{C}$  gHMBC and  $^1\text{H}$ - $^1\text{H}$  gDQCOSY spectra related to the methylene olefinic protons at  
 10  $\delta_{\text{H}}$  4.82 and 4.58, and two methyl groups at  $\delta_{\text{H}}$  1.70 and 1.03.  $^1\text{H}$ - $^{13}\text{C}$  long-range correlations  
 11 of protons at 4.82, 4.58 and 1.70 ppm revealed the presence of an isopropenyl spin system  
 12 linked to a methyne group at  $\delta_{\text{C}}$  52.5 (Fig. 3c). The second  $\text{CH}_3$  group ( $\delta_{\text{C}}$  16.6 and  $\delta_{\text{H}}$  1.03)  
 13 expectedly showed correlations with quaternary carbon atom at  $\delta_{\text{C}}$  39.5 ppm, while further  
 14 extension of this structural fragment was made possible by the cross peaks with an =CH-  
 15 group ( $\delta_{\text{C}}$  150.0 and  $\delta_{\text{H}}$  5.83), as well as, with the mentioned methine carbon at  $\delta_{\text{C}}$  52.5.  
 16 Unfortunately, the proton of the =CH- group showed long-range  $^1\text{H}$ - $^{13}\text{C}$  coupling to only a  
 17 quaternary carbon atom at  $\delta_{\text{C}}$  39.5 ppm. However, this proton coupled to a proton ( $^1\text{H}$ - $^1\text{H}$   
 18 gDQCOSY) in the range 4.88-4.95 ppm corresponding to both remaining methylene olefinic  
 19 protons.  
 20



21  
 22

23 **Fig. 3.** (a) Expansion of the  $^1\text{H}$ - $^{13}\text{C}$  gHMBC spectrum of sample **A** with key cross peaks  
 24 marked with appropriate coloring to match that in **b** and **c**. (b) and (c) structural fragments  
 25 with marked observed  $^1\text{H}$ - $^{13}\text{C}$  gHMBC interactions (dashed colored arrows). Gray double  
 26 ended arrow represents a  $^1\text{H}$ - $^1\text{H}$  gDQCOSY interaction.

27 Thus, one should expect a vinyl group in the structure of the sesquiterpene aldehyde,  
 28 *i.e.* it should be expected to display a characteristic ABX spin system. The chemical shifts  
 29 and coupling constants of the multiplets that appeared at 5.83 and 4.88-4.95 ppm were solved  
 30 by the use of WinDNMR software,<sup>21</sup> and the simulated spectrum is given as a supplementary  
 31 file (Fig. S1). The established 2,4-dimethylhexa-1,5-diene-3,4-diyl fragment is frequently  
 32 encountered in sesquiterpenes of elemene and related skeletons.

33 Judging from the molecular formula of the aldehyde, a total of five unsaturations  
 34 should be accounted for. This means that the fifth unsaturation (alongside the three C=C and  
 35 one C=O) should correspond to a ring. The up to now assigned carbon and hydrogen



1 resonances make up a total of 12 carbon and 14 hydrogen atoms, while 2 additional protons  
2 from CH groups ( $\delta_C$  52.5 and  $\delta_H \approx 2.10$ , and  $\delta_C$  36.5 and  $\delta_H \approx 2.55$ ) located only by the data  
3 from 2D spectra. Thus, the identity-chemical shifts of 3 carbon and 6 hydrogen atoms still  
4 remained undetermined. The only unassigned intense peaks in the DEPT135 spectrum were  
5 those from CH<sub>2</sub> groups at  $\delta_C$  39.7, 32.8, 29.7 and 26.8. Thus, it appeared likely that the  
6 missing carbons and protons of the aldehyde were three CH<sub>2</sub> groups. However, as these  
7 methylene protons resonated at high field, their precise chemical shift assignment was  
8 rendered impossible due to severe overlap, both mutual and with impurity signals (Fig. 2b).

9 Although the above given detailed analysis of the NMR spectra of mixture **A**  
10 provided valuable data it did not result in a specific complete proposition of the structure of  
11 the aldehyde. Next, having in mind that the sesquiterpene contains an aldehyde group, which  
12 is considered a good Lewis base, it was decided to try to simplify the proton spectrum in the  
13 high field region by an NMR-monitored titration with LSR. The formation of an adduct with  
14 LSR could possibly enable the assignment of the proton from the CH group at  $\delta_C$  36.5 ( $\delta_H \approx$   
15 2.55) attached to the acrolein moiety-the coordination site of LSR, *i.e.* a significant downfield  
16 shift should be expected. Eu(fod)<sub>3</sub> was chosen as LSR because it combines the maximum  
17 shift capacity with minimum broadening of the shifted resonances, good solubility in  
18 chloroform with absence of interfering chelate resonances in the usual range of NMR  
19 frequencies.<sup>8</sup> The incremental addition of Eu(fod)<sub>3</sub> resulted in a great simplification of the <sup>1</sup>H  
20 NMR spectrum of sample **A** as a number of signals were observed to move to lower field.  
21 While the shifts of the first fragment (Fig. 3b) proton signals, located near the coordination  
22 site, were expected, the effect of Eu(fod)<sub>3</sub> on the protons from the vinyl, isopropenyl and the  
23 second CH group ( $\delta_C$  52.5 and  $\delta_H \approx 2.10$ ) from the second fragment were unforeseen (Fig. 4).

24 At first glance, the most striking changes were: the mutual separation achieved for the  
25 protons from the =CH<sub>2</sub> end of the vinyl group and the clean detachment of two CH groups  
26 from the complex upfield region ( $\delta_H < 3$  ppm) in the unshifted reference spectrum. At the  
27 approximate molar ratio [Eu(fod)<sub>3</sub>]/[aldehyde] = 0.45, two well separated doublet of doublets  
28 at  $\delta_H$  5.06 ( $J = 17.5, 1.3$  Hz) and  $\delta_H$  5.00 ( $J = 10.8, 1.3$  Hz), that together with a doublet of  
29 doublets at  $\delta_H$  6.03 ( $J = 17.5, 10.8$  Hz) formed the ABX spin system of the vinyl group, could  
30 be observed (Fig. 4, Table 1). In alkenes, *trans* coupling generally results in larger coupling  
31 constants compared to *cis* coupling and with geminal coupling being by far the smallest.  
32 Thus, the proton (labelled H<sub>b</sub>) that had a slightly higher  $\delta_H$  occupied the *trans* position  
33 relative to the =CH- proton. The location of protons from the two CH groups was facilitated  
34 by the fact that the effect of LSR is approximately equal for a <sup>13</sup>C nucleus as for a proton in  
35 approximately the same location (the same  $\Delta\delta$  values in ppm), *i.e.* directly attached to the  
36 carbon.<sup>6</sup> The CH groups could be easily located from the shifted gHMQC spectrum (at molar  
37 ratio 0.45) as <sup>13</sup>C NMR spectra changed much less dramatically than the proton spectra did,  
38 since the chemical shift range of the <sup>13</sup>C nucleus is much larger. At the molar ratio 0.45, the  
39 proton from the CH group closer to the coordination site appeared as a broad triplet of triplets  
40 at  $\delta_H$  4.74 ( $J \approx 12, 3$  Hz), while the proton from the more remote CH group resonated at  $\delta_H$   
41 2.68 as a broad doublet of doublets ( $J = 12.8, 3.0$  Hz).

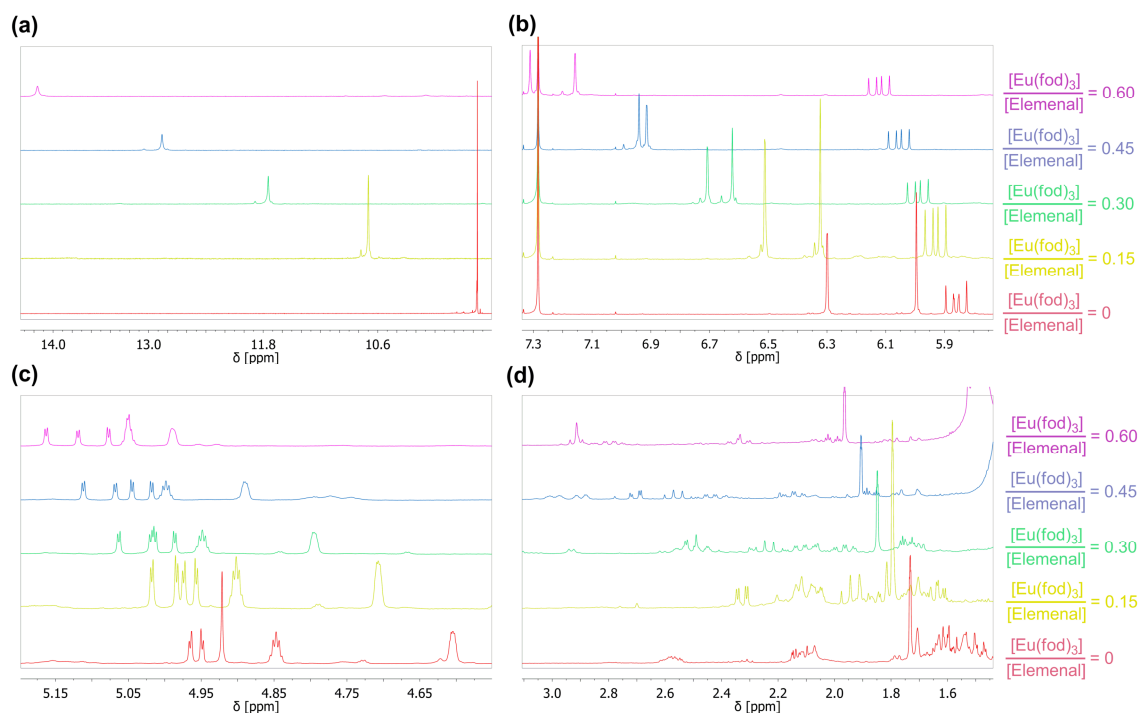


**Fig. 4.** The shifts of signals after incremental additions of  $\text{Eu}(\text{fod})_3$  corresponding to: (a) the aldehyde proton, the olefinic protons with (b)  $\delta_{\text{H}} > 5.8$  ppm and (c)  $\delta_{\text{H}} < 5$  ppm in the unshifted spectrum, and (d) the enlargement of the area with the aliphatic protons with  $\delta_{\text{H}}$  between 1.45 and 2.60 ppm in the unshifted spectrum.

Furthermore, the shifted gHMBC spectrum (at the molar ratio of 0.45) revealed the presence of three pairs of diastereotopic protons, *i.e.* three  $\text{CH}_2$  groups as: (i) protons at  $\delta_{\text{H}}$  2.95 and 2.41 that correlated with the carbon at  $\delta_{\text{C}}$  28.0, (ii) protons at  $\delta_{\text{H}}$  2.87 and 2.53 that correlated with the carbon at  $\delta_{\text{C}}$  33.9, and (iii) protons at  $\delta_{\text{H}}$  2.12 and 1.84 attached to the carbon with  $\delta_{\text{C}}$  40.3 (Table 1). Such a segregation of the mentioned diastereotopic protons was crucial for the completion of the structure of the sesquiterpene aldehyde since the presence of a  $(\text{C})_2\text{CH}-\text{CH}_2-\text{CH}(\text{C})-\text{CH}_2-\text{CH}_2-\text{C}(\text{C})_3$  closed spin system was finally clearly evident from the  $^1\text{H}-^1\text{H}$  gDQCOSY spectrum (molar ratio 0.45; Fig. 5a). The established connectivity was also sustained by appropriate correlations in  $^1\text{H}-^{13}\text{C}$  gHMBC spectrum (molar ratio 0.45). This system linked fragments 1 and 2, making up a cyclohexane ring and completing the elemene skeleton of the aldehyde. The observed multiplicity of the  $\text{CH}_2$  group signals was in agreement with the existence of an 1,3,4,4-tetrasubstituted cyclohexane ring: geminal and axial-axial couplings on one side, and equatorial-equatorial and axial-equatorial on the other, are both of very similar magnitude ( $J_{\text{gem}} \approx J_{\text{aa}}$  and  $J_{\text{ee}} \approx J_{\text{ae}}$ ) giving rise to very complex pseudo-shaped signals (Table 1).

**Table 1.**  $^1\text{H}$  and  $^{13}\text{C}$  NMR data for elemental and  $\text{Eu}(\text{fod})_3$ -elemental complex at molar ratio 0.45 and experimental  $\Delta\text{Eu}$  values for certain protons

Position	Elemental		[Eu(fod) <sub>3</sub> ]/[Elemental] = 0.45		$\Delta\text{Eu}$
	$\delta_{\text{H}}$ [ppm]	$\delta_{\text{C}}$ [ppm]	$\delta_{\text{H}}$ [ppm]	$\delta_{\text{C}}$ [ppm]	
1	5.83 (1H, m)	150.0	6.03 (1H, dd, $J = 17.5, 10.8$ Hz)	150.2	0.41
2	4.92 <sup>a</sup> 4.93 <sup>a</sup>	110.1	<b>a:</b> 5.00 (1H, dd, $J = 10.8, 1.3$ Hz) <b>b:</b> 5.06 (1H, dd, $J = 17.5, 1.3$ Hz)	110.2	0.23 0.27
3	<b>a:</b> 4.82 (1H, pseudo-quint, $J = 1.6$ Hz) <b>b:</b> 4.58 (1H, pseudo-dq, $J = 1.6, 0.8$ Hz)	112.2	<b>a:</b> 4.97 (1H, m) <b>b:</b> 4.86 (1H, m)	112.5	0.32 0.61
4	/	147.4	/	147.8	/
5	2.14 <sup>a</sup>	52.5	2.68 (1H, br dd, $J = 12.8, 3.0$ Hz)	53.1	1.23
6	$\approx 1.59$ (2H) <sup>b</sup>	32.8 <sup>c</sup>	<b>e:</b> 2.87 (1H, pseudo-dt, $J = 12.9, 3.2$ Hz) <b>a:</b> 2.53 (1H, pseudo-q, $J = 12.5$ Hz)	33.9	/
7	2.58 <sup>a</sup>	36.5	4.74 (1H, br tt, $J \approx 12, 3$ Hz)	38.6	4.95
8	<b>e:</b> $\approx 1.62$ <sup>b</sup> <b>a:</b> $\approx 1.46$ <sup>b</sup>	26.8	<b>e:</b> 2.95 (1H, br pseudo-d quint $J = 13.5, 3$ Hz) <b>a:</b> 2.41 (1H, pseudo-qd, $J = 13.5, 3.4$ Hz)	28.0	/
9	<b>e:</b> $\approx 1.47$ <sup>b</sup> <b>a:</b> $\approx 1.56$ <sup>b</sup>	39.7	<b>e:</b> 1.84 (1H, pseudo-dt, $J = 13.4, 3.4$ Hz) <b>a:</b> 2.12 (1H, pseudo-td, $J = 13.4, 3.6$ Hz)	40.3	/
10	/	39.5	/	40.0	/
11	/	155.0	/	<sup>d</sup>	/
12	9.53 (1H, br s)	194.5	12.83 (1H, s)	207.2	7.55
13	<b>a:</b> 6.27 (1H, br d, $J = 0.7$ Hz) <b>b:</b> 5.97 (1H, br s)	132.9	<b>a:</b> 6.89 (1H, br d, $J = 0.7$ Hz) <b>b:</b> 6.91 (1H, s)	135.3	1.39 2.13
14	1.03 (3H, br s)	16.6	1.38 (3H, br s)	17.0	0.74
15	1.70 (3H, dd, $J = 1.6, 0.8$ Hz)	24.9	1.88 (3H, dd, $J = 1.6, 0.8$ Hz)	25.0	0.36

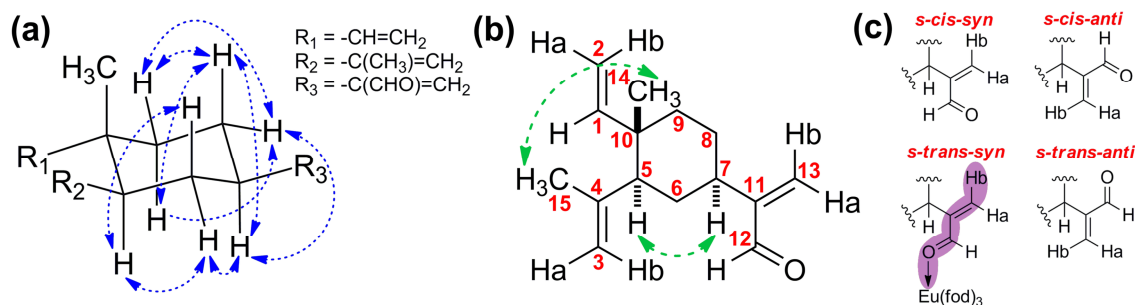
<sup>a</sup> Chemical shift is determined by extrapolation of proton plot to  $[\text{Eu}(\text{fod})_3]/[\text{Elemental}] = 0$ ;

<sup>b</sup> Chemical shift is estimated from a cross-peak in the gHMQC spectrum;

<sup>c</sup> Chemical shift were assigned based on the value of appropriate induced chemical shift;

<sup>d</sup> The determination of this chemical shift value was hindered due to extensive signal broadening.

1 A literature survey revealed that an aldehyde with the elemene skeleton like the one  
 2 just established had been previously described but has a rather restricted occurrence in nature.  
 3 This sesquiterpene aldehyde named elemenal had been previously isolated in pure state only  
 4 from *Thujopsis dolabrata* Stieb. et Zucc.<sup>22</sup> and *Saussurea lappa* Clarke<sup>23</sup> root essential oils.  
 5 The structure of elemenal was initially proposed based on limited spectral data (UV-Vis, IR  
 6 and <sup>1</sup>H NMR (at 90 Hz); available at the time) and afterwards confirmed, along with the  
 7 determination of its absolute configuration, by comparison with an authentic semisynthetic  
 8 sample obtained from (-)-β-elemene. The relative stereochemistry of our elema-1,3,11(13)-  
 9 trien-12-al was inferred to be the same as that of the previously reported elemenal from the  
 10 very informative shifted NOESY spectrum of sample A (Fig. 5b). The presence of Eu(fod)<sub>3</sub>  
 11 (at 0.45 molar ratio) did not result in the disappearance of nOe, most probably because the  
 12 main *modus operandi* of this LSR was a pseudocontact or dipolar interaction (a through space  
 13 effect) - which originates from a secondary magnetic field, that is usually anisotropic,  
 14 generated by the paramagnetic cation (as opposed to contact shifts (e.g. a through-bonds  
 15 effect) - which arise from delocalization of the unpaired electron-spin through bonds to the  
 16 nuclei affected).<sup>3</sup>  
 17



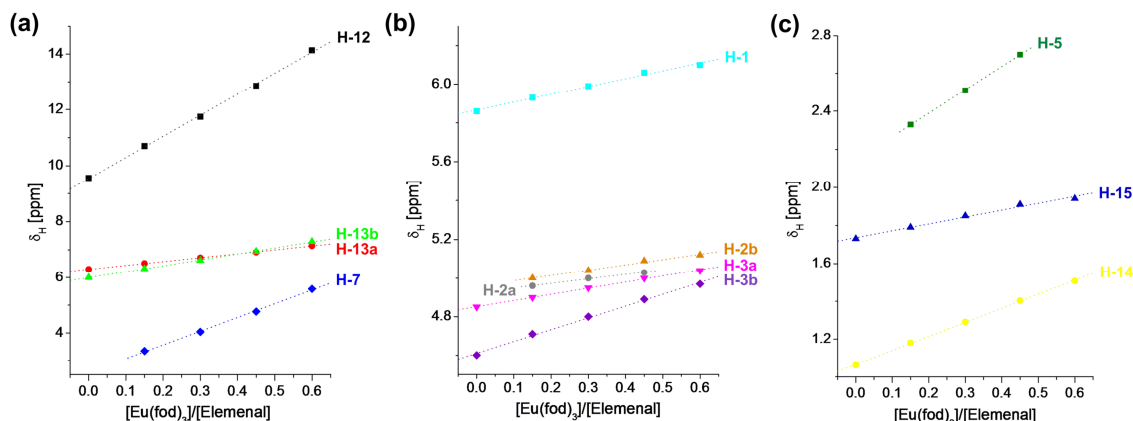
18  
 19

20 **Fig. 5.** (a) The most important <sup>1</sup>H-<sup>1</sup>H gDQCOSY cross-peaks used for the structure  
 21 elucidation of the sesquiterpene aldehyde. (b) The structure of elemenal with a numberings  
 22 scheme of its carbon atoms and the crucial nOe cross-peaks used for the determination of its  
 23 relative stereochemistry. (c) Four possible conformations of the methacrolein moiety. The  
 24 zig-zag oriented σ-system in the *s-trans-syn* conformation, through which the largest extent  
 25 of electron spin density transfer could be expected, is denoted by violet shading.

26 Furthermore, elemenal had also been tentatively identified (based solely on the  
 27 fragmentation pattern visible in its mass spectrum, since there was no MS published till de  
 28 Kraker *et al.*<sup>24</sup>) as a minor constituent of essential oils obtained from *Origanum onites* L.,<sup>25</sup>  
 29 *Teucrium pestalozzae* Bois<sup>26</sup> and *Perovskia scrophulariifolia* Bunge<sup>27</sup> aerial parts, and *Abies*  
 30 *cilicica* subsp. *cilicica* (Ant. et Kotschy) Carr. young shoots.<sup>28</sup> It was claimed to be identified  
 31 by mass spectral comparison (GC-MS, but no isolation) as a constituent of essential oils from  
 32 *Mentha pulegium* L. aerial parts,<sup>29</sup> *Zingiber neesatum* (Graham) Ramamoorthy<sup>30</sup> and  
 33 *Zingiber zerumbet* (L.) Smith rhizome.<sup>31</sup> However, the latest reinvestigation of *Saussurea*  
 34 *lappa* Clarke fresh root essential oil and extract composition indicated that (-)-elemenal,  
 35 along with (-)-β-elemene and (-)-elema-1,3,11(13)-trien-12-ol, is most possibly a heat-  
 36 induced artefact formed from the corresponding germacrene derivatives by Cope  
 37 rearrangement during drying of the roots, and/or manufacture of the oil and/or GC analysis.<sup>24</sup>

38 Although a large amount of information can be gleaned by a visual analysis of a series  
 39 of spectra obtained from incremental additions of LSR, the information could be sometimes  
 40 more conveniently expressed in graphical form, usually as a plot of induced shift vs. the ratio  
 41 of [LSR]/[substrate] and generally good linear correlation is noted for the range 0.2-0.6 mole

1 ratio.<sup>2</sup> The slope of the plot is called shift gradient ( $\Delta E_u$ ) and its value is generally greater if a  
 2 proton is near to the coordination site of LRS. In our case, the highest value of the induced  
 3 chemical shift was observed for the protons from the aldehyde group and C(7)-H group (at  $\delta_C$   
 4 36.5 and  $\delta_H \approx 2.58$ ) with  $\Delta E_u$  of 7.55 and 4.95, respectively, followed by the protons from the  
 5 conjugated  $=CH_2$  group with  $\Delta E_u$  1.39 and 2.13 for H-13a and H-13b protons, respectively  
 6 (Fig. 6a, Table 1).



8  
 9  
 10 **Fig. 6.** The chemical shift vs. the ratio of the shift reagent and elemental plots obtained from  
 11 the incremental addition of  $Eu(fod)_3$  to elemental for: (a) the protons closest to the  
 12 coordination site, (b) the remaining olefinic protons and (c) for the protons that resonated at  
 13 the high field region.

14  
 15 The geminal protons H-13a and H-13b displayed a so-called "signal crossover"  
 16 phenomenon, since the induced shift plot of H-13b crossed over the plot of H-13a (Fig. 6a).  
 17 Usually this occurrence could be explained by the fact that H-13b is closer to the binding site  
 18 of  $Eu(fod)_3$  when compared to H-13a.<sup>1</sup> However, according to its greater  $\delta_H$ , H-13a has  
 19 already been assigned to be *cis* to the aldehyde group, and thus should be closer to the  
 20 coordinating site of the paramagnetic cation and, thus, should feel a stronger secondary  
 21 magnetic field and have a greater lanthanide-induced shift. Moreover, previous studies on  
 22 methacrylaldehyde indeed showed that a proton *cis* to the aldehyde group had a somewhat  
 23 greater lanthanide-induced shift.<sup>32,33</sup> As there are two possible conformers for this system (*s-*  
 24 *cis* and *s-trans* around C-11-C-12), if the methacrylic moiety were to adopt the *s-trans*  
 25 conformation,  $Eu(fod)_3$  bonded to the oxygen atom would be placed further away and this  
 26 would result in a lesser effect of the secondary magnetic field on H-13a (this orientation of  
 27 the aldehyde group is in agreement with the NOESY cross-peak observed for CHO proton  
 28 and H-13a in the shifted spectra).

29 Another conformational issue that can be inferred from the shifted spectra is the  
 30 relative orientation around C-11-C-7 bond. Since the influence of the secondary magnetic  
 31 field falls away sharply with distance, the drastically higher  $\Delta E_u$  value (4.95) of H-7  
 32 compared to the methylene protons H-13a and H-13b (1.39 and 2.13; Fig. 6a, Table 1)  
 33 suggests that elemental- $Eu(fod)_3$  complex should adopt such a conformation (*s-trans* around  
 34 C-11-C-12 and a *syn* orientation of H-7 and CHO around C-11-C-7) in which this proton (H-  
 35 7) is in very close proximity to the paramagnetic ion (Fig. 5c). Moreover, another pro  
 36 argument for this conformation is that the methylene proton H-3b also felt a stronger  
 37 influence of the paramagnetic ion than its geminal proton H-3a (Fig. 6b; Table 1), having  
 38 almost two-fold higher  $\Delta E_u$  value, and being possible only in the *s-trans-syn* conformation

1 orienting  $\text{Eu}(\text{fod})_3$  towards the mentioned isopropenyl group. However, these conclusions are  
2 strictly valid only for the europium complex, not for the free aldehyde since the observed  
3 anisotropic influence of CHO on H-13a is only possible in the *s-cis* conformation.

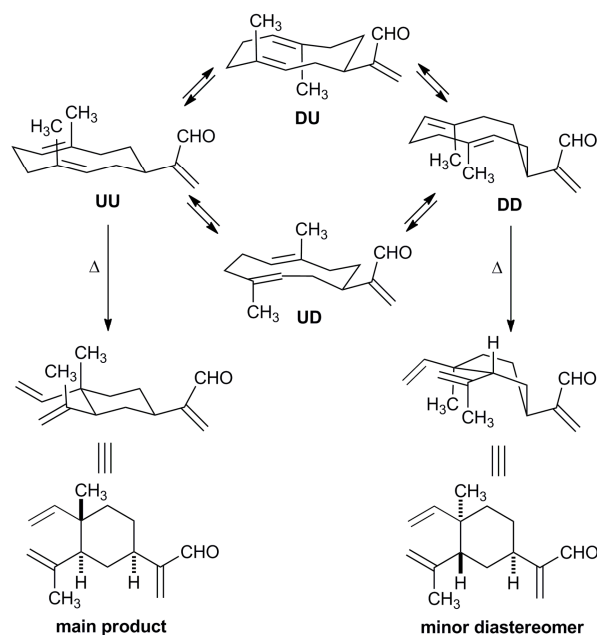
4 Generally, it is believed that with lanthanides a small degree (*ca.* 1%) of contact shift  
5 (*e.g.* a through-bonds effect) is usually possible, particularly for protons attached to the  
6 carbons nearest the lone-pair-bearing atoms.<sup>3</sup> Thus, the second part of the explanation of this  
7 unusual phenomenon (H-13b *trans* to the aldehyde group in an  $\alpha,\beta$ -unsaturated carbonyl  
8 system has a higher  $\Delta\text{Eu}$  value than the *cis* H-13a) could be the greater degree of contact shift  
9 for H-13b in our LSR adduct. It has been suggested that a contact shift is significant for  
10 aromatic systems where the presence of conjugation may increase the electron delocalization,  
11 thus increasing the degree of contact contribution to the observed shift of resonances for the  
12 protons throughout the molecule.<sup>3</sup> In a similar manner, electron spin density could be  
13 transferred through a properly oriented (zig-zag)  $\sigma$ -system electrons of an  $\alpha,\beta$ -unsaturated  
14 carbonyl system, as present in the *s-trans* conformation in our case, and affect more the  
15 proton *trans* to the aldehyde group due to better orbital overlap (Fig. 5c).

16 Plotting the spectral data obtained during the incremental addition studies turned out  
17 to be additionally advantageous. For example,  $\delta_{\text{H}}$  values from clustered, highly overlapped  
18 signals (no LSR present) could be estimated by extrapolation of proton plots to  
19  $[\text{Eu}(\text{fod})_3]/[\text{substrate}] = 0$ .<sup>1</sup> In fact,  $\delta_{\text{H}}$  values for protons H-2a, H-2b, H-5 and H-7 could  
20 probably be determined more accurately from the y-axis cut-off of the proton plots (Fig. 6;  
21 Table 1) than from <sup>1</sup>H NMR spectrum shown in Fig. 2a, or from 2D spectra, since the precise  
22 chemical shift positions of these proton signals are uncertain either due to mutual overlap of  
23 these signals or the presence of signals arising from the impurities (Fig. 2b).

24 As mentioned above, elemenes are believed to be formed by a Cope rearrangement of  
25 the corresponding germacrane. In solution, germacrane could adopt any of the four distinct  
26 conformations that allow a [3,3]-sigmatropic rearrangement to occur, namely UU, UD, DU,  
27 and DD with an assumption that the isopropenyl or related substituent is large enough to  
28 ensure its equatorial or pseudo-equatorial position on the cyclodecadiene ring (Fig. 7).<sup>34</sup> Cope  
29 rearrangement is a stereospecific reaction that generally proceeds *via* a chair-like transition  
30 state and this geometric requirement is fulfilled in UU or DD forms of the specific  
31 germacrane.<sup>24</sup> Both experimental data and computational studies point to the UU (up-up)  
32 conformation, in which the two methyl groups and the pseudo-equatorial substituent adopt  
33 positions on the top face of the crossed cyclodecadiene ring, as the most stable one and  
34 predominant in the conformational equilibrium.<sup>34</sup>

35 Thus, the Cope rearrangement should preferably proceed *via* this conformation and it  
36 is considered that the "naturally occurring"  $\beta$ -elemene (and its derivatives as well) adopt a  
37 chair conformation with the relative stereochemistry of the groups on the cyclohexane ring  
38 that was governed by the stereochemistry in the starting germacrene and the geometric  
39 demands of the cyclic transition state (Fig. 7).<sup>24,35</sup> The main destabilizing factor in this  
40 proposed conformation (designated as **Conf-1**) for  $\beta$ -elemene and its derivatives is the *syn*-  
41 pentane interaction between the angular methyl group and the methyl group from the  
42 isopropenyl substituent (Fig. 8a). Our MM2 calculations for elemenal revealed that the  
43 destabilizing effect of the *syn*-pentane interaction would be decreased for *ca.* 2 kcal mol<sup>-1</sup> if  
44 =CH<sub>2</sub> end of the isopropenyl group was oriented in parallel to the angular methyl group (as in  
45 conformer **Conf-2**; Fig. 8b). Conversely, NOESY cross-peaks between the mentioned methyl  
46 groups, as well as the occurrence of a four-bond vinyl-allylic proton spin-coupling, between  
47 H-5 and H-3b (H-3b is a pseudo-doublet quintets; Fig. 5b; Fig. 8d; Table 1), and not H-5 and  
48 H-3a (H-3a is a pseudo-quintet), clearly point to the orientation of the isopropenyl group as in  
49 conformer **Conf-1**, *i.e.* a U relationship between H-5 and H-3b. Furthermore, in the more  
50 stable conformer **Conf-2** only a W-type coupling of the allylic H-5 and the vinyl H-3a proton

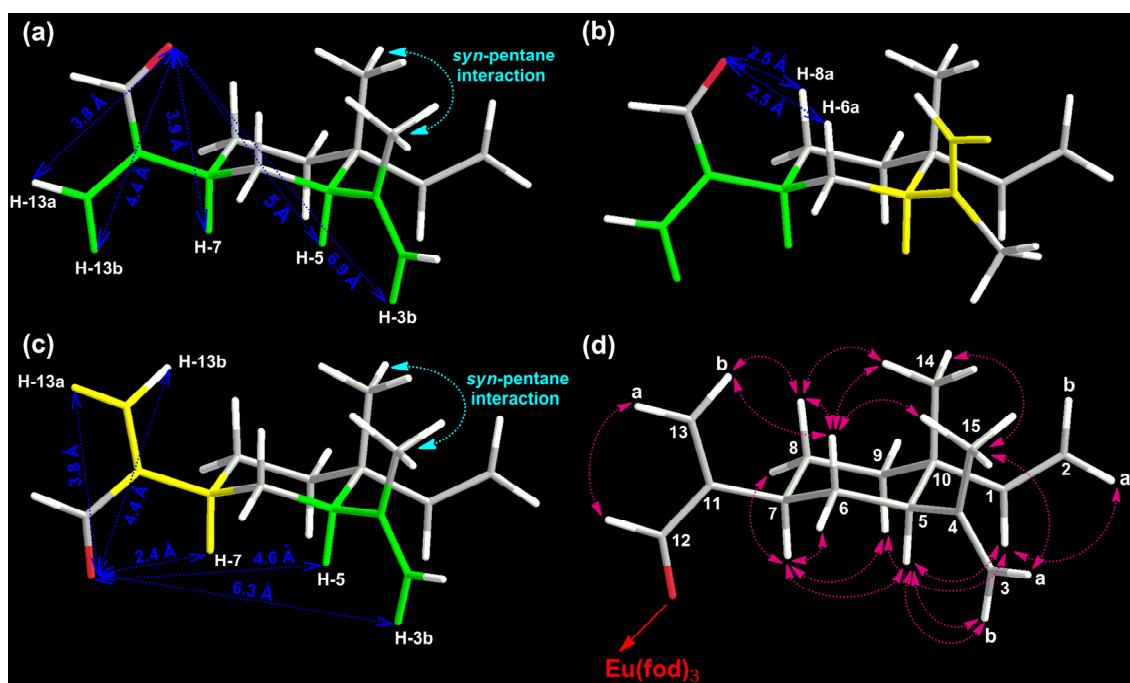
1 is expected ( ${}^4J_{\sigma} > 0$  Hz). Conformer **Conf-1** does not permit this coupling to be observed  
 2 ( ${}^4J_{\sigma,\pi} \approx 0$  Hz) as the dihedral angle  $\theta$  between these vinyl and allylic C-H bonds is very close  
 3 to  $180^\circ$  ( $175.7^\circ$ ).<sup>36</sup>



5  
 6  
 7 **Fig. 7.** Possible conformations of germacradialenol fixed by the equatorial or pseudo-equatorial  
 8 position of the relatively large substituent in the position 7 of the 10-membered ring. The  
 9 conformers are denoted as UU, UD, DU, and DD in reference to the U (up) and D (down)  
 10 orientations of C-14 and C-15 methyl groups. Both UU and DD conformations could undergo  
 11 Cope rearrangement, however, the predominant UU conformation would yield the main  
 12 stereoisomer of elemenal, whereas the less stable DD conformation would give the minor  
 13 diastereoisomer of elemenal.

14  
 15 Interestingly, in the both mentioned conformers so far (**Conf-1** and **Conf-2**; Figs. 8a  
 16 and 8b), MM2 calculations predict, as the most energetically favorable, the *s-trans*  
 17 conformation of the methacrylic fragment and the *anti*-orientation of the CHO group with  
 18 respect to H-7 on the cyclohexane ring. However, a noted small vinyl-allylic coupling ( $J =$   
 19  $0.7$  Hz) between H-13a (*cis* to the aldehyde group) and H-7 in both shifted and non-shifted  
 20 spectra implies that the aldehyde group is oriented *syn* to H-7 (conformer **Conf-3**; Fig. 8c) in  
 21 both the free aldehyde and the europium complex. **Conf-3** displays a value of the dihedral  
 22 angle  $\theta$  between the vinyl and allylic C-H bonds very close to zero ( $\theta = 0.9^\circ$ ), so a  
 23 characteristic W-coupling should be expected. On the other hand, conformers **Conf-1** and  
 24 **Conf-2**, with the corresponding dihedral angle close to  $180^\circ$  ( $179.4^\circ$ ), do not support this  
 25 coupling (the value of  ${}^4J_{\sigma,\pi}$  should be close to zero in this case). Additionally, conformers  
 26 **Conf-1** and **Conf-2** should give rise to U-coupling of H-13b (*trans* to the aldehyde group)  
 27 and H-7 (Figs. 8a and 8b) which is not observed. Furthermore, in the *anti*-orientation of the  
 28 aldehyde group (**Conf-1** and **Conf-2**), the distance between H-13a and H-7 from the aldehyde  
 29 oxygen atom are almost the same, ( $3.8$  Å and  $3.9$  Å, respectively), and these protons should,  
 30 thus, experience a very similar effect of the secondary magnetic field. However, as mentioned  
 31 above the very opposite was noted since the experimentally determined  $\Delta E_u$  values for these  
 32 protons differed significantly. As previously put forward, the greater magnitude of the  
 33 induced shift for H-7 could be only explained by the *s-trans-syn* conformation of the

1 elemental-Eu(fod)<sub>3</sub> complex in which this proton is in close proximity to the paramagnetic ion  
 2 and, indeed, according to MM2 calculations, the proton H-7 should be considerably closer  
 3 than H-12a to the coordinating site (2.3 Å compared to 3.8 Å; **Conf-3**, Fig. 8c).  
 4



5  
6

7 **Fig. 8.** Plausible conformations of elemental denoted throughout the text as **Conf-1** (a), **Conf-**  
 8 **2** (b) and **Conf-3** (c) with the indicated distances of certain protons to the aldehyde oxygen  
 9 atom, as well as, the observed NOESY cross-peaks presented on conformation **Conf-3** that is  
 10 most likely adopted in the elemental-Eu(fod)<sub>3</sub> complex (d). The possible vinyl-allylic W-  
 11 couplings are marked in yellow, while U-couplings are marked in green color.  
 12

13 MM2 calculations also predict that conformer **Conf-3** should be only 0.5-0.6 kcal  
 14 mol<sup>-1</sup> higher in strain energy than conformer **Conf-1**. Another fact which does not favor the  
 15 predominance of **Conf-1**, in our case, is the relatively small magnitude of lanthanide-induced  
 16 shift detected for axial H-6 and H-8. These shifts should be quite higher since the distance of  
 17 these protons from the Eu(fod)<sub>3</sub> binding site is around 2.5 Å in **Conf-1** (Fig. 8a). Similar  
 18 considerations stand for other protons (Table 1; Fig. 8), as well. Thus, the herein presented  
 19 experimental data (vinyl-allylic couplings, NOESY cross-peaks and  $\Delta E$  values)  
 20 unequivocally support **Conf-3** as the major conformer of elemental-Eu(fod)<sub>3</sub> complex.  
 21

22 In order to additionally justify the conclusions regarding the stereochemistry of the  
 23 elemental-Eu(fod)<sub>3</sub> complex, we performed a conformational analysis using the lanthanide  
 24 probe method.<sup>37,38</sup> An internal Cartesian coordinate was set up with the carbonyl oxygen at  
 25 the origin while the C=O bond defined the negative *z*-axis. Subsequently, the location of the  
 26 europium ion could be specified by the bond length Eu–O (*r<sub>o</sub>*), the bond angle Eu–O–C(12),  
 27 ( $\alpha_o$ ) and the dihedral angle Eu–O–C(12)–C(13) ( $\beta_o$ ).<sup>37</sup> Throughout the calculation, the  
 28 optimal europium ion position, the substrate coordinates, as well as its geometry (as in **Conf-**  
 29 **3**), were kept constant and the europium ion was allowed to move (to give the best match  
 30 with the experimental data), *i.e.* its coordinates were changed incrementally using the  
 31 ChemBio 3D Ultra 12.0 software package. The value of the dihedral angle was set to 180°  
 32 in order to ensure the co-planarity of europium and the methacrolein moiety (that was  
 mandatory for a good electron spin density transfer), while the bond angle  $\alpha_o$  was varied from



110° to 130° (to provide minimal deviations from the properly zig-zag oriented  $\sigma$ -system) and the bond length  $r_o$  was in the range between 2.30 and 2.56 Å. For each location of the lanthanide ion, the variable geometrical factors  $(3\cos^2\theta_i - 1)/r_i^3$  in the McConnell-Robertson equation were calculated for all the observed nuclei ( $i$ ) of the substrate (where  $r_i$  is the distance between the lanthanide ion and the  $i$ -th nucleus, and  $\theta_i$  is the angle between the vector corresponding to  $r_i$  and the vector  $r_o$  representing the Ln–coordination center bond). Then the calculated values ( $\Delta_{\text{cal}}$ ) for all tested europium positions were plotted against the observed values ( $\Delta\text{Eu}$ ).<sup>38</sup> The highest correlation coefficient ( $R^2 = 0.9980$ ; Fig. S2) was found when europium was located at  $r_o = 2.328$  Å,  $\alpha_o = 120^\circ$  and  $\beta_o = 180^\circ$  (Fig. S3). Since the McConnell-Robertson equation can be applied only to nuclei where contact interactions are negligible,<sup>38</sup> the values for H-12, H-13a and H-13b were excluded from these fittings (*e.g.* this pseudocontact model predicted a higher induced shift value ( $\Delta_{\text{cal}}$ ) for H-13a when compared to H-13b, while the experimental values were the other way around). The observed induced shift values ( $\Delta\text{Eu}$ ) for protons H-12, H-13a and H-13b could be regarded as to represent the combination (in the first approximation, a simple sum) of the dipolar or pseudocontact ( $\Delta\text{Eu}_{\text{dip}}$ ) and contact ( $\Delta\text{Eu}_{\text{contact}}$ ) terms. Thus, an estimation of the share of the contact and dipolar contributions for these protons could be performed based on their  $\Delta_{\text{cal}}$  values and the linear regression equation  $\Delta\text{Eu}_{\text{dip}} = -0.28 + 251.82 \times \Delta_{\text{cal}}$  obtained for the most likely conformation (Fig. S3). In this way, we found that, for example, for proton H-13b a significant fraction of the observed induced chemical shift ( $\Delta\text{Eu}_{\text{total}} = 2.13$ ) could be attributed to the contact interaction ( $\Delta\text{Eu}_{\text{contact}} \approx 0.62$ ).

The instability of germacrenes, *i.e.* its susceptibility to heat-induced (*e.g.* steam distillation or high temperature drying of plant material) Cope rearrangement which yield the corresponding elemenes, is one of the main reasons terpenes with an elemene skeleton are considered to have an artefactual origin and not a natural one.<sup>24</sup> We found that elemenal, isolated from *I. helenium* root essential oil, did not adopt the most stable conformation (**Conf-2**). The established conformation (**Conf-3**) displays the orientation of the angular methyl group and methyl group from the isopropenyl substituent on the cyclohexane ring which strictly reflects the spatial relationship of these groups on the 10-membered ring in the most stable conformation (UU) of the corresponding germacradiene from which Cope rearrangement most probably occurred. Interestingly, there were no peaks in NMR spectra that supported the existence of elemenal (even in a small percentage) in the most stable conformation (**Conf-2**), most probably because of the high energy barrier for the rotation around C-4–C-5 bond. Furthermore, de Kraker and co-workers<sup>24</sup> found that during the heating of germacradienal, a small amount of another artefact which is a diastereomer of elemenal was also formed and this was explained by the fact that Cope rearrangement had also occurred through the less stable DD conformation. This diastereomer of elemenal was also noted in sample **A** after a closer inspection of the TIC chromatogram (RI = 1546). All these facts go in favor that elemenal is highly related to the corresponding germacradienal but these do not exclude either a thermal or a biosynthetic link.

Interestingly,  $\beta$ -elemene is widely considered as a potential novel natural anticancer plant drug and some formulations for pharmacological uses based on this compound have been patented and are currently in application for clinical studies in the United States.<sup>39</sup> A recent study revealed that  $\beta$ -elemenal was appreciably more potent than  $\beta$ -elemene in suppressing nonsmall cell lung cancer growth and proliferation. Thus,  $\beta$ -elemenal may have great potential as an anticancer alternative to  $\beta$ -elemene in treating lung cancer and other tumors.<sup>40</sup>

## Conclusion

1 In conclusion, herein, we reported on the identification of a rare sesquiterpene  
2 elemental directly from minute amounts of a complex mixture (without the availability of a  
3 pure sample of the aldehyde) achieved by the aid an NMR titration of the mixture with a  
4 lanthanide-induced shift reagent. The incremental addition of Eu(fod)<sub>3</sub> led to a simplification  
5 of NMR spectra in terms of signal overlap and removal of chemical shift degeneracy,  
6 allowing the mining of crucial data from the shifted NMR spectra. 2D-NMR spectra (<sup>1</sup>H-<sup>1</sup>H-  
7 COSY, NOESY, HSQC and HMBC) of the sample mixed with Eu(fod)<sub>3</sub> proved to be  
8 particularly valuable in this respect. The addition of the shift reagent shortened the time  
9 needed to acquire <sup>13</sup>C NMR and 2D spectra from 5 mg of the mixture, while it did not cause  
10 any serious line broadening or loss of nOe. Alongside the total NMR assignments of  
11 elemental, the data obtained from the shifted spectra enabled a detailed assessment of the  
12 conformation that this sesquiterpene aldehyde adopts in its complex with Eu(fod)<sub>3</sub>. Providing  
13 this much data, this new approach in structure elucidation promises to be of great help in the  
14 NMR analysis of complex samples comprising of several compounds.

## 15 16 **Experimental section**

### 17 18 **Chemicals and reagents**

19  
20 All chemicals and solvents were of analytical grade and used without further  
21 purification. Diethyl ether, *n*-hexane, anhydrous magnesium sulphate, neryl isobutanoate,  
22 geraniol, isobutanoic acid, tris(6,6,7,7,8,8,8-heptafluoro-2,2-dimethyl-3,5-  
23 octanedionato)europium(III) (Eu(fod)<sub>3</sub>), tetramethylsilane and deuterated chloroform were  
24 purchased from Sigma-Aldrich (St Louis, MS, USA). Dicyclohexylcarbodiimide and 4-  
25 dimethylaminopyridine were supplied by Merck (Darmstadt, Germany). Geranyl  
26 isobutanoate was synthesized from geraniol and isobutanoic acid by a Steglich procedure,  
27 utilizing dicyclohexylcarbodiimide and 4-dimethylaminopyridine.<sup>41</sup> Chromatographic  
28 separations were carried out using silica gel 60 (particle size distribution 20–45 μm) obtained  
29 from Carl Roth GmbH + Co.KG (Karlsruhe, Germany).

### 30 31 **Plant material**

32  
33 Roots of *I. helenium* were collected in the beginning of April 2014 in vicinity of the  
34 town Svrljig in South-eastern Serbia. A voucher specimen was deposited with the Herbarium  
35 of the Faculty of Science and Mathematics, University of Niš, under the accession number  
36 GM0114.

### 37 38 **Essential oil – extraction and fractionation**

39  
40 *Inula helenium* root essential oil was obtained by hydrodistillation (air-dried plant  
41 material) using the original Clevenger-type apparatus according to a previously described  
42 method.<sup>16</sup> The yield of the essential oil was 1.3% (w/w).

43 A sample of the oil (2.1 g) was subjected to "dry flash" column chromatography on  
44 silica gel (particle size 20–45 μm). Pure *n*-hexane (100 mL) was used as the eluent for the  
45 first three fractions (**I-III**), followed by 1% (v/v) diethyl ether in *n*-hexane (fraction **IV**, 100  
46 mL), 2% (v/v) diethyl ether in *n*-hexane (fractions **V** and **VI**, 100 mL) and finally pure  
47 diethyl ether (fraction **VII**, 200 mL). The solvent was removed *in vacuo* and the obtained  
48 fractions submitted to GC–MS analyses. Fractions **III** and **IV** contained the unknown  
49 sesquiterpene aldehyde as a major component and were pooled together (sample **A**, 4.8 mg).

**Elemenal:** RI (DB-5) = 1578; MS (EI, 70 eV),  $m/z$  218 ( $M^+$ , 2.1%), 217 (0.6, M – H), 203 (14.9, M – CH<sub>3</sub>), 200 (3.5, M – H<sub>2</sub>O), 189 (9.6, M – CHO), 175 (15.5), 161 (28.7), 147 (21.7), 133 (18.8), 121 (27.1), 119 (28), 107 (37.7), 105 (34.6), 95 (38.6), 93 (47), 91 (52), 81 (100), 79 (64.3), 77 (34.1), 68 (35), 67 (60.6), 55 (32.7), 53 (40.9), 41 (49.7), 39 (28.2). For <sup>1</sup>H and <sup>13</sup>C NMR data see Table 1.

**Geranyl isobutanoate:** RI (DB-5) = 1506; MS (EI, 70 eV),  $m/z$  224 ( $M^+$ , 0.2%), 181 (0.1, M – C<sub>3</sub>H<sub>7</sub>), 154 (2.3), 136 (16.7), 121 (29), 107 (8.2), 93 (46.1), 80 (19.8), 69 (100, (CH<sub>3</sub>)<sub>2</sub>C=CCH<sub>2</sub>), 53 (9.4), 41 (41);  $\delta_H$  (400 MHz; CDCl<sub>3</sub>; (CH<sub>3</sub>)<sub>4</sub>Si) 1.16 (6H, d,  $J$  = 7.0 Hz, (CH<sub>3</sub>)<sub>2</sub>CHC=O), 1.60 (3H, br s, -CH<sub>2</sub>-CH=C(CH<sub>3</sub><sup>cis</sup>)CH<sub>3</sub><sup>trans</sup>), 1.68 (3H, br d,  $J$  = 1.0 Hz, -CH<sub>2</sub>-CH=C(CH<sub>3</sub><sup>cis</sup>)CH<sub>3</sub><sup>trans</sup>), 1.70 (3H, br s, -O-CH<sub>2</sub>-CH=C(CH<sub>3</sub>)-CH<sub>2</sub>-), 2.01–2.07 (2H, m, -O-CH<sub>2</sub>-CH=C(CH<sub>3</sub>)-CH<sub>2</sub>), 2.07–2.15 (2H, m, -CH<sub>2</sub>-CH=C(CH<sub>3</sub><sup>cis</sup>)CH<sub>3</sub><sup>trans</sup>), 2.54 (1H, hept,  $J$  = 7.0 Hz, (CH<sub>3</sub>)<sub>2</sub>CHC=O), 4.58 (2H, br d,  $J$  = 7.0 Hz, -O-CH<sub>2</sub>-CH=C(CH<sub>3</sub>)-CH<sub>2</sub>-), 5.08 (1H, pseudo-t hept,  $J$  = 6.8, 1.4 Hz, -CH<sub>2</sub>-CH=C(CH<sub>3</sub><sup>cis</sup>)CH<sub>3</sub><sup>trans</sup>) and 5.33 (1H, pseudo-t sext,  $J$  = 7.0, 1.3 Hz, -O-CH<sub>2</sub>-CH=C(CH<sub>3</sub>)-CH<sub>2</sub>-);  $\delta_C$  (101 MHz; CDCl<sub>3</sub>; (CH<sub>3</sub>)<sub>4</sub>Si) 177.3 ((CH<sub>3</sub>)<sub>2</sub>CHC=O), 142.0 (O-CH<sub>2</sub>-CH=C(CH<sub>3</sub>)-CH<sub>2</sub>-), 131.9 (-CH<sub>2</sub>-CH=C(CH<sub>3</sub><sup>cis</sup>)CH<sub>3</sub><sup>trans</sup>), 124.0 (-CH<sub>2</sub>-CH=C(CH<sub>3</sub><sup>cis</sup>)CH<sub>3</sub><sup>trans</sup>), 118.8 (O-CH<sub>2</sub>-CH=C(CH<sub>3</sub>)-CH<sub>2</sub>-), 61.4 (O-CH<sub>2</sub>-CH=C(CH<sub>3</sub>)-CH<sub>2</sub>-), 39.7 (O-CH<sub>2</sub>-CH=C(CH<sub>3</sub>)-CH<sub>2</sub>-), 34.2 ((CH<sub>3</sub>)<sub>2</sub>CHC=O), 26.5 (-CH<sub>2</sub>-CH=C(CH<sub>3</sub><sup>cis</sup>)CH<sub>3</sub><sup>trans</sup>), 25.8 (-CH<sub>2</sub>-CH=C(CH<sub>3</sub><sup>cis</sup>)CH<sub>3</sub><sup>trans</sup>), 19.2 ((CH<sub>3</sub>)<sub>2</sub>CHC=O), 17.8 (-CH<sub>2</sub>-CH=C(CH<sub>3</sub><sup>cis</sup>)CH<sub>3</sub><sup>trans</sup>) and 16.6 (O-CH<sub>2</sub>-CH=C(CH<sub>3</sub>)-CH<sub>2</sub>-).

**Neryl isobutanoate:** RI (DB-5) = 1482; MS (EI, 70 eV),  $m/z$  224 ( $M^+$ , 0.2%), 181 (0.1, M – C<sub>3</sub>H<sub>7</sub>), 154 (2.2), 136 (13.9), 121 (34.1), 107 (8.6), 93 (68.3), 80 (26.8), 69 (100, (CH<sub>3</sub>)<sub>2</sub>C=CCH<sub>2</sub>), 53 (9.9), 41 (53.1);  $\delta_H$  (400 MHz; CDCl<sub>3</sub>; (CH<sub>3</sub>)<sub>4</sub>Si) 1.16 (6H, d,  $J$  = 7.0 Hz, (CH<sub>3</sub>)<sub>2</sub>CHC=O), 1.60 (3H, br s, -CH<sub>2</sub>-CH=C(CH<sub>3</sub><sup>cis</sup>)CH<sub>3</sub><sup>trans</sup>), 1.68 (3H, br s, -CH<sub>2</sub>-CH=C(CH<sub>3</sub><sup>cis</sup>)CH<sub>3</sub><sup>trans</sup>), 1.76 (3H, pseudo-q,  $J$  = 1.3 Hz, -O-CH<sub>2</sub>-CH=C(CH<sub>3</sub>)-CH<sub>2</sub>-), 2.03–2.15 (4H, m, -CH<sub>2</sub>-CH<sub>2</sub>-), 2.53 (1H, hept,  $J$  = 7.0 Hz, (CH<sub>3</sub>)<sub>2</sub>CHC=O), 4.56 (2H, br d,  $J$  = 7.2 Hz, -O-CH<sub>2</sub>-CH=C(CH<sub>3</sub>)-CH<sub>2</sub>-), 5.10 (1H, pseudo-t hept,  $J$  = 6.9, 1.4 Hz, -CH<sub>2</sub>-CH=C(CH<sub>3</sub><sup>cis</sup>)CH<sub>3</sub><sup>trans</sup>) and 5.35 (1H, pseudo-t sext,  $J$  = 7.2, 1.3 Hz, -O-CH<sub>2</sub>-CH=C(CH<sub>3</sub>)-CH<sub>2</sub>-);  $\delta_C$  (101 MHz; CDCl<sub>3</sub>; (CH<sub>3</sub>)<sub>4</sub>Si) 177.3 ((CH<sub>3</sub>)<sub>2</sub>CHC=O), 142.4 (O-CH<sub>2</sub>-CH=C(CH<sub>3</sub>)-CH<sub>2</sub>-), 132.2 (-CH<sub>2</sub>-CH=C(CH<sub>3</sub><sup>cis</sup>)CH<sub>3</sub><sup>trans</sup>), 123.8 (-CH<sub>2</sub>-CH=C(CH<sub>3</sub><sup>cis</sup>)CH<sub>3</sub><sup>trans</sup>), 119.6 (O-CH<sub>2</sub>-CH=C(CH<sub>3</sub>)-CH<sub>2</sub>-), 61.1 (O-CH<sub>2</sub>-CH=C(CH<sub>3</sub>)-CH<sub>2</sub>-), 34.2 ((CH<sub>3</sub>)<sub>2</sub>CHC=O), 32.4 (O-CH<sub>2</sub>-CH=C(CH<sub>3</sub>)-CH<sub>2</sub>-), 26.8 (-CH<sub>2</sub>-CH=C(CH<sub>3</sub><sup>cis</sup>)CH<sub>3</sub><sup>trans</sup>), 25.8 (-CH<sub>2</sub>-CH=C(CH<sub>3</sub><sup>cis</sup>)CH<sub>3</sub><sup>trans</sup>), 23.6 (O-CH<sub>2</sub>-CH=C(CH<sub>3</sub>)-CH<sub>2</sub>-), 19.2 ((CH<sub>3</sub>)<sub>2</sub>CHC=O) and 17.8(-CH<sub>2</sub>-CH=C(CH<sub>3</sub><sup>cis</sup>)CH<sub>3</sub><sup>trans</sup>).

### Analytical and spectral analyses

**GC–MS analyses.** The GC–MS analyses of all samples (the essential oil and chromatographic fractions, standards) were repeated three times using a Hewlett-Packard 6890N gas chromatograph. The gas chromatograph was equipped with a fused silica capillary column DB-5 (5% phenylmethylsiloxane, 30m × 0.25 mm, film thickness 0.25 μm; Agilent Technologies, Santa Clara, CA, USA) and coupled with a 5975B mass selective detector from the same company. The injector and interface were operated at 250 and 300 °C, respectively. The oven temperature was raised from 70 to 290 °C at a heating rate of 5 °C/min and then isothermally held for 10min. Helium at 1.0 mL/min was used as a carrier gas. The samples, 1 μL of the corresponding solutions in diethyl ether (1:10, w/v), were injected in a pulsed split mode (the flow was 1.5 mL/min for the first 0.5 min and then set to 1.0 mL/min throughout the remainder of the analysis; split ratio 40:1). The mass selective detector was operated at the ionisation energy of 70 eV, in the 35–500 amu range, with a scanning speed of 0.34 s.

**NMR measurements.** All NMR spectra were recorded at 27 °C in deuterated chloroform with tetramethylsilane as the internal standard. Chemical shifts ( $\delta$ ) are reported in parts per million and referenced to tetramethylsilane ( $\delta_{\text{H}} = 0$  ppm) in  $^1\text{H}$  NMR spectra and/or to solvent protons (deuterated chloroform:  $\delta_{\text{H}} = 7.25$  ppm and  $\delta_{\text{C}} = 77$  ppm) in heteronuclear 2D spectra. Scalar couplings are reported in hertz (Hz). Samples (10 mg for geranyl and neryl isobutanoates, and a 4.8-mg fraction containing elemenal) were dissolved in 1 mL of deuterated chloroform, and 0.7 mL of the solution transferred into a 5 mm Wilmad, 528-TR-7 NMR tube.

The  $^1\text{H}$ - and  $^{13}\text{C}$  NMR spectra were recorded on a Bruker Avance III 400 MHz NMR spectrometer (Fällanden, Switzerland;  $^1\text{H}$  at 400 MHz,  $^{13}\text{C}$  at 101 MHz), equipped with a 5-mm dual  $^{13}\text{C}/^1\text{H}$  probe head. The  $^1\text{H}$  spectra were recorded with 16 scans, 1 s relaxation delay, 4 s acquisition time, 0.125 Hz digital FID resolution, 51 280 FID size, with 6410 Hz spectral width, and an overall data point resolution of 0.0003 ppm. The  $^{13}\text{C}$  spectra were recorded with Waltz 161H broadband decoupling, 12000 scans, 0.5 s relaxation delay, 1 s acquisition time, 0.5 Hz digital FID resolution, 65536 FID size, 31850 Hz spectral width, and an overall data point resolution of 0.005 ppm. Standard pulse sequences were used for 2D spectra.  $^1\text{H}$ - $^1\text{H}$  gDQCOSY and NOESY spectra were recorded at spectral widths of 5 kHz in both F2 and F1 domains; 1 K  $\times$  512 data points were acquired with 32 scans per increment and the relaxation delays of 2.0 s. The mixing time in NOESY experiments was 1 s. Data processing was performed on a 1 K  $\times$  1 K data matrix. Inverse detected 2D heteronuclear correlated spectra were measured over 512 complex points in F2 and 256 increments in F1, collecting 128 (gHMQC) or 256 ( $^1\text{H}$ - $^{13}\text{C}$  gHMBC) scans per increment with a relaxation delay of 1.0 s. The spectral widths were 5 and 27 kHz in F2 and F1 dimensions, respectively. The gHMQC experiments were optimized for C-H couplings of 125 Hz; the  $^1\text{H}$ - $^{13}\text{C}$  gHMBC experiments were optimized for long-range C-H couplings of 10 Hz. Fourier transforms were performed on a 512  $\times$  512 data matrix.  $\pi/2$  Shifted sine-squared window functions were used along F1 and F2 axes for all 2D spectra.

$\text{Eu}(\text{fod})_3$  was used as the lanthanide shift agent and four equimolar increments of  $\text{Eu}(\text{fod})_3$  were added to a 0.015 mol/dm<sup>3</sup> solution of the substrate in deuterated chloroform. The molar ratio of  $\text{Eu}(\text{fod})_3$  to elemenal was estimated to be in the range from 0 to 0.6. The reagents were dissolved by shaking and the spectra were recorded at 27 °C after dissolution.

### Computational methods

Geometry optimizations and calculation of the (thermodynamic) properties of elemenal were performed using the MM2 molecular mechanics force field method incorporated in ChemBio 3D Ultra 12.0 software package.

### Acknowledgements

The authors acknowledge the Ministry of Education, Science and Technological Development of Serbia for the financial support (Project No. 172061). This work is part of the PhD thesis of Marija S. Genčić supervised by Niko S. Radulović.

### References

1. J. P. Wineburg and D. Swern, *J. Am. Oil Chem. Soc.*, 1972, **49**, 267–273.
2. A. F. Cockerill, G. L. O. Davies, R. C. Harden and D. M. Rackam, *Chem. Rev.*, 1973, **73**, 552–588.
3. B. C. Mayo, *Chem. Soc. Rev.*, 1973, **2**, 49–74.

- 1 4. C. C. Hinckley, *J. Am. Chem. Soc.*, 1969, **91**, 5160–5162.
- 2 5. A. V. Turov, S. P. Bondarenko, A. A. Thachkuk and V. P. Khilya, *Rus. J. Org. Chem.*,
- 3 2005, **41**, 47–53.
- 4 6. O. A. Gansow, M. R. Willcott and R. E. Lenkinski, *J. Am. Chem. Soc.*, 1971, **93**, 4295–
- 5 4297.
- 6 7. C. C. Hinckley, M. R. Klotz and F. Patil, *J. Am. Chem. Soc.*, 1971, **93**, 2417–2420.
- 7 8. W. Kuhn and H. Rembold, *Z. Naturforsch. C*, 1977, **32**, 563–566.
- 8 9. T. Chakrabartty, G. Poddar and J. st. Pyrek, *Phytochemistry*, 1982, **21**, 1814–1816.
- 9 10. C. Seger, O. Hofer and H. Greger, *Monatsh. Chem.*, 2000, **131**, 1161–1165.
- 10 11. R. A. Schenato, É. M. dos Santos, P. F. B. Gonçcalves, B. S. M. Tenius, E. R. de
- 11 Oliveira, I. Caracelli and J. Zukerman-Schpector, *Magn. Reson. Chem.*, 2003, **41**, 53–60.
- 12 12. D. Ristorcelli, F. Tomi and J. Casanova, *Flavour Frag. J.*, 1998, **13**, 154–158.
- 13 13. N. Baldovini, F. Tomi and J. Casanova, *Phytochem. Anal.*, 2003, **14**, 241–244.
- 14 14. D. A. Lanfranchi, F. Tomi and J. Casanova, *Phytochem. Anal.*, 2010, **21**, 597–601.
- 15 15. A. D. Wright, G. M. König and O. Sticher, *Phytochem. Anal.*, 1992, **3**, 73–79.
- 16 16. J. Orjala, A. D. Wright, T. Rali and O. Sticher, *Nat. Prod. Lett.*, 1993, **2**, 231–236.
- 17 17. G. M. König and A. D. Wright, *Magn. Reson. Chem.*, 1995, **33**, 178–183
- 18 18. B. D. Flockhart and D. Thorburn Burns, *Pure Appl. Chem.*, 1987, **59**, 915–926.
- 19 19. Z. Z. Stojanović-Radić, L. R. Čomić, N. S. Radulović, P. D. Blagojević, M. Denić, A. B.
- 20 Miltojević, J. Rajković and T. M. Mihajilov-Krstev, *Eur. J. Clin. Microbiol. Infect. Dis.*,
- 21 2012, **31**, 1015–1025.
- 22 20. N. S. Radulović, M. S. Denić and Z. Z. Stojanović-Radić, *Phytochem. Anal.*, 2014, **25**,
- 23 75–80.
- 24 21. H. J. Reich, *J. Chem. Educ.*, 1995, **72**, 1086.
- 25 22. S. Itô, K. Endo, H. Honma and K. Ota, *Tetrahedron Lett.*, 1965, **6**, 3777–3781.
- 26 23. B. Maurer and A. Grieder, *Helv. Chim. Acta*, 1977, **60**, 2177–2190.
- 27 24. J-W. de Kraker, M. C. R. Franssen, A. de Groot, T. Shibata and H. J. Bouwmeester,
- 28 *Phytochemistry*, 2001, **58**, 481–487.
- 29 25. D. Biondi, P. Cianci, C. Gerad, G. Ruberto and M. Piattelli, *Flavour Frag. J.*, 1993, **8**,
- 30 331–337.
- 31 26. K. H. C. Baser, B. Demirçakmak and H. Duman, *J. Essent. Oil Res.* 1997, **9**, 545–549.
- 32 27. Kh. R. Nuriddinov, K. Kh. Khodzimatov, Kh. N. Aripov, T. Ozek, B. Demirchakmak and
- 33 K. H. C. Basher. *Chem. Nat. Compd.*, 1997, **33**, 299–300.
- 34 28. E. Bağci, K. H. C. Başer, M. Kürkcüoğlu, T. Babaç and S. Çelik, *Flavour Frag. J.*, 1999,
- 35 **14**, 47–49.
- 36 29. H. Boukhebt, A. N. Chaker, H. Belhadj, F. Sahli, M. Ramdhani, H. Laouer and D.
- 37 Harzallah, *Der Pharmacia Lettre*, 2011, **3**, 267–275.
- 38 30. B. Sabulal, M. Dan, A. J. John, R. Kurup, S. P. Chandrika and V. George, *Flavour Frag.*
- 39 *J.*, 2007, **22**, 521–524.
- 40 31. S. Baby, M. Dan, A. R. M. Thaha, A. J. Johnson, R. Kurup, P. Balakrishnapillai and C. K.
- 41 Lim, *Flavour Frag. J.*, 2009, **24**, 301–308.
- 42 32. G. Montaudo, V. Librando, S. Caccamese and P. Maravigna, *J. Am. Chem. Soc.*, 1973,
- 43 **95**, 6365–6370.
- 44 33. P. Finocchiaro, A. Recca, P. Maravigna and G. Montaudo, *Tetrahedron*, 1974, **30**, 4159–
- 45 4169.
- 46 34. J. A. Faraldos, S. Wu, J. Chappell and R. M. Coates, *Tetrahedron*, 2007, **63**, 7733–7742.
- 47 35. K. Takeneda, *Tetrahedron*, 1974, **30**, 1525–1534.
- 48 36. E. W. Garbisch, *J. Am. Chem. Soc.*, 1964, **86**, 5561–5564.
- 49 37. F. Inagaki and T. Miyazawa, *Prog. Nucl. Mag. Res. Sp.*, 1980, **14**, 67–111.

- 1 38. O. Hofer, in *Topics in Stereochemistry*, ed. N. L. Allinger and E. L. Eliel, John Wiley &
- 2 Sons, Inc., Hoboken, 1976, vol. 9, ch. 3, pp. 111–197.
- 3 39. A. F. Barrero, M. M. Herrador, J. F. Quílez del Moral, P. Arteaga, N. Meine, M. C. Pérez-
- 4 Morales and J. V. Catalán, *Org. Biomol. Chem.*, 2011, **9**, 1118–1125.
- 5 40. Q. Q. Li, G. Wang, F. Huang, J. M. Li, C. F. Cuff and E. Reed, *Med. Oncol.*, 2013, **30**,
- 6 488–498.
- 7 41. N. S. Radulović, M. Denić, Z. Z. Stojanović-Radić and D. Skropeta, *J. Am. Oil Chem.*
- 8 *Soc.*, 2012, **89**, 2165–2185.